# Experimental Proposal for J-PARC

# Search for a nuclear $\bar{\mathrm{K}}$ bound state $K^{-}pp$ in the $d(\pi^{+}, K^{+})$ reaction

T. Nagae*, K. Imai, H. Fujioka, A. Okamura, M. Moritsu,
H. Asano, S. Adachi, Y. Sada, H. Sugimura
*Kyoto University,*
*Kitashirakawa, Sakyo-ku, Kyoto 606-8502, Japan*

T. Takahashi, M. Naruki, S. Ishimoto, A. Toyoda
*IPNS, KEK,*
*1-1 Oho, Tsukuba, Ibaraki 305-0801, Japan*

K. Hosomi, T. Koike, K. Miwa, K. Shirotori, H. Tamura
*Tohoku University,*
*6-3 Aoba, Aramaki, Aoba-ku, Sendai 980-8578, Japan.*

June 16, 2009

**Abstract**

We propose to produce the $K^{-}pp$ bound state via the $d(\pi^{+}, K^{+})$ reaction. So far, the $(\pi^{+}, K^{+})$ reaction has been successfully used for $\Lambda$ hypernuclear spectroscopy at 1.05 GeV/$c$, at which $\pi^{+}$ incident momentum the $\Lambda$ production cross section at forward angles has the maximum. By increasing the incident momentum at around 1.5 GeV/$c$, we can produce a lot of $\Lambda(1405)$'s. Then, we can expect the formation of a $\bar{\mathrm{K}}$ nucleus with the $\Lambda(1405)$ as a doorway. In this experiment, we are going to use a liquid deuterium target to produce the $K^{-}pp$ system via the $d(\pi^{+}, K^{+})$ reaction. Two-proton tagging method is applied to remove quasifree hyperon production backgrounds.

## 1 Motivation and Purpose

The first experimental evidence for a $\bar{\mathrm{K}}$ bound state $K^{-}pp$ was claimed by the FINUDA group at DAΦNE in 2005 [1]. Japanese collaborators of the FINUDA group significantly contributed to this analysis. We observed the $\Lambda - p$ pairs emitted in back-to-back from the stopped $K^{-}$ absorption on $^{6}$Li, $^{7}$Li, and $^{12}$C targets. The invariant mass of the $\Lambda - p$ system was much smaller than the mass of the $K^{-} + p + p$ system (Fig. 1). Thus, it could be evidence that the $K^{-}pp$ bound system is formed in the stopped $K^{-}$ absorption in the surface region of nuclei and decays into the $\Lambda - p$ pair. The binding energy of $115^{+6}_{-5}(\mathrm{stat})^{+3}_{-4}(\mathrm{syst})$ MeV and the width of $67^{+14}_{-11}(\mathrm{stat})^{+2}_{-3}(\mathrm{syst})$ MeV were obtained. Later, the mass shift of the $\Lambda - p$ pairs has been confirmed in a new data set of much improved statistics. Further, we have found there is not such a large mass shift in the $K^{-} + p + n$ system decaying into $\Lambda + n$ and $\Sigma^{-} + p$ [2].

*Spokesperson

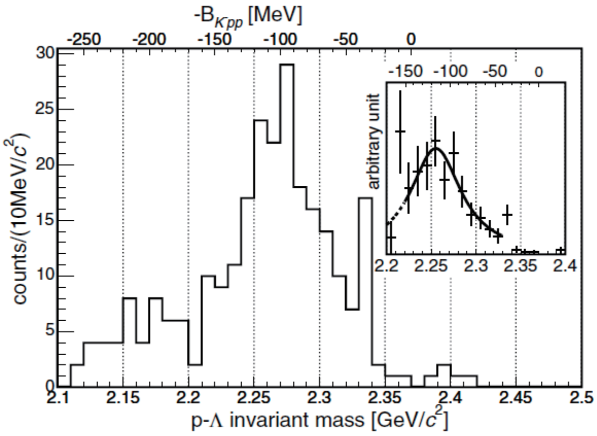


Figure 1: Invariant mass of a $\Lambda$ and a proton in back-to-back correlation ($\cos\theta^{Lab} \leq -0.8$) from light targets before the acceptance correction. The inset shows the result after the acceptance correction [1].

However, the reaction mechanism to produce such a deeply-bound $K^-pp$ system in the stopped $K^-$ absorption is not known well. Therefore, as for the interpretation of this mass shift, other interpretations [3] could not be excluded.

Since the $K^-pp$ system must be the most simplest nuclear $\bar{\mathrm{K}}$ bound states, if existed, a lot of work to theoretically examine the existence of the $K^-pp$ system has been carried out by using reliable few-body techniques. Faddeev calculations have been carried out by Shevchenko *et al.* [4] and by Ikeda and Sato [5]. Yamazaki and Akaishi [6, 7], and Doté *et al.* [8] have calculated based on variational approaches. All of these calculations have confirmed that the $K^-pp$ bound state must exist with the binding energy of 20 to 70 MeV depending on the $\bar{\mathrm{K}}N$ interaction models used in the calculations. However, it depends on the width of the bound state whether the state is experimentally observed as a peak structure or not. There is a tendency that the width is as large as ~100 MeV when the binding energy is small. It should be noted that the observed state could be a bound state of $\Lambda(1405)$ [9] rather than a $\bar{\mathrm{K}}$ bound state.

After the FINUDA observation, there have been several reports on possible signals of the $K^-pp$ in heavy ion collisions by FOPI group [10], in antiproton-$^4$He annihilation by OBELIX group [11], and in proton-proton collision by DISTO group [12]. However, the obtained binding energies etc. are not conclusive.

Therefore, it is of vital importance to experimentally confirm the existence of the $K^-pp$ bound state observed by the FINUDA group. Already at J-PARC, an experiment, E15 (Spokespersons: M. Iwasaki and T. Nagae), to search for the $K^-pp$ in $^3\mathrm{He}(K^-, n)$ reaction is approved as one of the Day-1 experiments at the Hadron Experimental Hall. While a high-intensity $K^-$ beam at 1 GeV/$c$ is required in E15, here we propose an alternative way to use a $\pi^+$ beam at 1.5 GeV/$c$. Thus, the demand for the primary beam intensity is modest in this experiment.

The first idea of a possible existence of $\bar{\mathrm{K}}NN$ bound states was proposed by Nogami [13] almost half a century ago, just after the discovery of $\Lambda(1405)$ [14].

However, such a recent trend to investigate the $\bar{\mathrm{K}}$ nuclear bound states had been initiated by the work of Akaishi and Yamazaki [16, 17, 15]. They predicted the possible presence of discrete nuclear bound states of $\bar{\mathrm{K}}$ in few-body nuclear systems. The binding energies and widths of few-body systems involving a $\bar{\mathrm{K}}$ were calculated from $\bar{\mathrm{K}}$N interactions which were constructed so as to account for the $\bar{\mathrm{K}}$N scattering lengths, the K$^-$-p atomic shift and the energy and width of $\Lambda(1405)$ under the assertion that $\Lambda(1405)$ is a bound state of $\bar{\mathrm{K}}$N. It became clear that the strong attraction of the $I = 0$ $\bar{\mathrm{K}}$N interaction ($\bar{\mathrm{K}}\mathrm{N}^{I=0}$) plays an important role in accommodating deeply bound states in proton-rich systems, where the $\bar{\mathrm{K}}\mathrm{N}^{I=0}$ attractive force is so strong that it overcomes the nuclear incompressibility and contracts the surrounding nuclear medium, thus producing enormously dense nuclear systems. Since the binding energies are large in some cases, the main decay channel of the $I = 0$ $\bar{\mathrm{K}}$N to $\Sigma + \pi$ is closed energetically, and additionally, the channel to $\Lambda + \pi$ is forbidden by the isospin selection rule. Thus, these deeply bound states are expected to have narrow widths. Very deep and narrow bound states, ${}^{3}_{\bar{\mathrm{K}}}\mathrm{H}(T = 0) \equiv \mathrm{K}^- \otimes {}^3\mathrm{He} + \bar{\mathrm{K}}^0 \otimes {}^3\mathrm{H}$ $(T = 0)$ and ${}^{4}_{\bar{\mathrm{K}}}\mathrm{H} \equiv \mathrm{K}^- \otimes {}^4\mathrm{He}$, with $\bar{\mathrm{K}}$ binding energies of 108 and 86 MeV and widths of 20 and 34 MeV, respectively, were predicted. The relation between these bound states and $\Lambda(1405)$ together with calculated $\mathrm{K}^-$ potentials is shown in Fig. 2. The contribution of additional non-pionic decay channels (i.e., two-nucleon absorption of $\mathrm{K}^-$) to the width is estimated to be around 12 MeV [15].

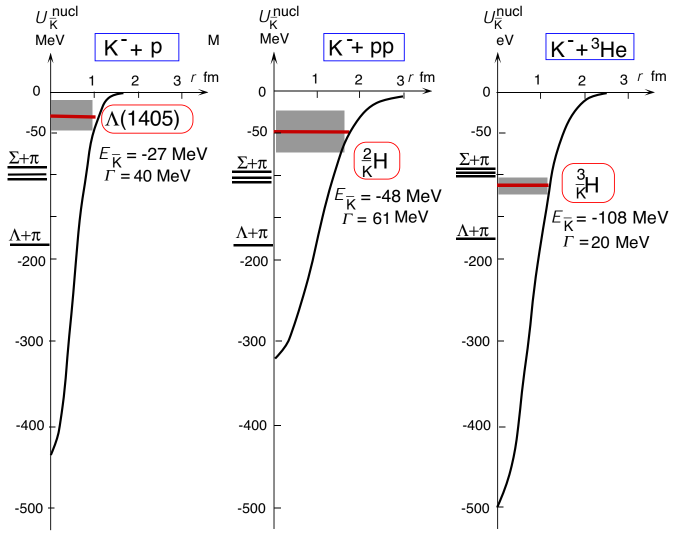


Figure 2: Calculated $\bar{\mathrm{K}}$N and $\bar{\mathrm{K}}$-nucleus potentials and bound levels [6]: $\Lambda(1405)$, ${}^{2}_{\bar{\mathrm{K}}}\mathrm{H}$ and ${}^{3}_{\bar{\mathrm{K}}}\mathrm{H}$ for $\mathrm{K}^-$p, $\mathrm{K}^-$pp and $\mathrm{K}^-$ppn systems, respectively. The nuclear contraction effect is taken into account. The shaded zones indicate the widths. The $\Sigma\pi$ and $\Lambda\pi$ emission thresholds are also shown.

In view of the situation that $\Lambda(1405)$ and these $\bar{\mathrm{K}}$ nuclei are bound states which are accommodated in $\mathrm{K}^-$ potentials, it is readily recognize that a nuclear $\bar{\mathrm{K}}$ system is nothing but "dissolved" $\Lambda^*$ states. Therefore, the formation of a $\Lambda^*$ in a nucleus as a "seed" will lead to the production of $\bar{\mathrm{K}}$ bound states. In other words, the $\Lambda^*$ produced in a nucleus can serve as a "doorway" toward $\bar{\mathrm{K}}$ bound states. The problem is how to produce $\Lambda^*$ in a nucleus and how to identify produced $\bar{\mathrm{K}}$ bound states. Yamazaki and Akaishi pointed out that the $(\pi^+,\mathrm{K}^+)$ (or similarly, $(\mathrm{K}^-,\pi^-)$) would lead to the production and detection of $\bar{\mathrm{K}}$ bound states [6].

## 2 Structure of $K^-pp$

Yamazaki and Akaishi studied theoretically the $\mathrm{K}^-$pp system ($={}^{2}_{\bar{\mathrm{K}}}\mathrm{H}$), the lightest nuclear system which may be called a *strange dibaryon* [6]. It may also be named a *nuclear kaonic hydrogen molecule.* Although the p-p system (${}^2$He) is unbound, the presence of a $\bar{\mathrm{K}}$ attracts two protons to form a bound state with $B = 48$ MeV and $\Gamma = 61$ MeV. This state is lying more deeply than $\Lambda(1405)$, but still above the $\Sigma\pi$ threshold, as shown in Fig. 2. This situation is intuitively understood in terms of the number of $\bar{\mathrm{K}}\mathrm{N}^{I=0}$ $(= 3/2)$ and the number of $\bar{\mathrm{K}}\mathrm{N}^{I=1}$ $(= 1/2)$.

The optical potential obtained for the $\mathrm{K}^-$pp system is

$$U^{\mathrm{opt}}(r) = (-300.0 - i\,70.0)\exp[-(r/1.09\ \mathrm{fm})^2]\ \mathrm{MeV}, \tag{1}$$

whereas the interaction for K$^-$p (namely, for $\Lambda(1405)$) is

$$V_{\bar{K}N}^{I=0}(r) = (-595.0 - i\,83.0)\exp[-(r/0.66\text{ fm})^2]\text{ MeV}. \quad (2)$$

The rms relative momentum of the K$^-$-p in $\Lambda(1405)$ is calculated to be 270 MeV/c, and the rms radius of the K$^-$ from the proton is 1.31 fm (0.86 fm from the c.m.). The density distributions of the K$^-$ and the protons in the K$^-$pp system were calculated from the above potential. The average distances of the K$^-$ from the center of p-p and from the proton are found to be 1.36 and 1.18 fm, respectively. The average distance between the two protons (averaged over the K$^-$ distribution) is 1.90 fm. Namely, in the K$^-$pp system, the inter-nucleon distance is similar to the ordinary one at the normal nuclear density. This is much smaller than the p-n distance in a deuteron (3.90 fm).

The other members of the K$^-$NN strange dibaryon system, namely, K$^-$nn and K$^-$d, are found to be unbound or much less bound. This result is understood because the interaction in K$^-$nn is $2 \times \bar{\mathrm{K}}\mathrm{N}^{I=1}$ on unbound $n-n$. In K$^-d$ the nucleus is bound, but the interaction is $(1/2)\bar{\mathrm{K}}\mathrm{N}^{I=0} + (3/2)\bar{\mathrm{K}}\mathrm{N}^{I=1}$, too weak to bind K$^-d$ below the $\Lambda(1405) + \mathrm{n}$ threshold. A naive argument in terms of an iso-doublet of $\Lambda^*$-N regarding $\Lambda^*$ as a structureless particle would lead to a totally different result.

# 3 Production through the $(\pi^+, K^+)$ reaction

D.W. Thomas *et al.*[18] studied the strange particle production from $\pi^-$p interactions at 1.69 GeV/$c$ with a hydrogen bubble chamber. In this measurement, three-body final states $\Sigma^\pm\pi^\mp K^0$, $\Sigma^{-}_{0}\pi^{0}_{-}K^+$, and $\Lambda\pi^{-}_{0}K^{+}_{0}$ were examined. In particular, the $\Lambda(1405)$ was clearly identified with about 400 events in the invariant mass spectrum of $\Sigma^\pm$ and $\pi^\mp$ as shown in Fig. 3; and the spin, mass, and width were determined. In fact, this is one of the two measurements clearly identified the $\Lambda(1405)$. The other one is that in the $K^-p$ reaction at 4.2 GeV/$c$[19] with about 1000 events.

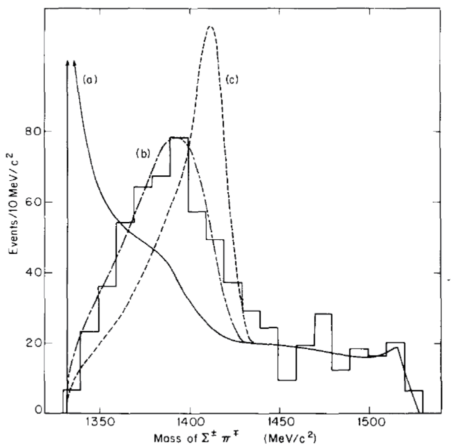


Figure 3: Mass distribution of $\Sigma^\pm\pi^\mp$[18]. The curves are based on some old theoretical analyses.

From an analysis on this $\Sigma^\pm\pi^\mp$ mass spectrum, they estimated the $\Lambda(1405)$ production was 46% of the total events, while they attributed remaining 43% to the phase space background and 8% and 3% to $\Sigma(1385)$ and $\Lambda(1520)$.

The differential cross section for $\pi^-p \to \Lambda(1405)K^0$ was also obtained as shown in Fig. 4. From this figure, the production cross section of $\Lambda(1405)$ in the $\pi^+n \to K^+\Lambda(1405)$ in the very forward direction is estimated to be 5$\mu$b/sr in the c.m. system assuming isospin symmetry, which amounts to $\approx$60$\mu$b/sr in the lab. system.

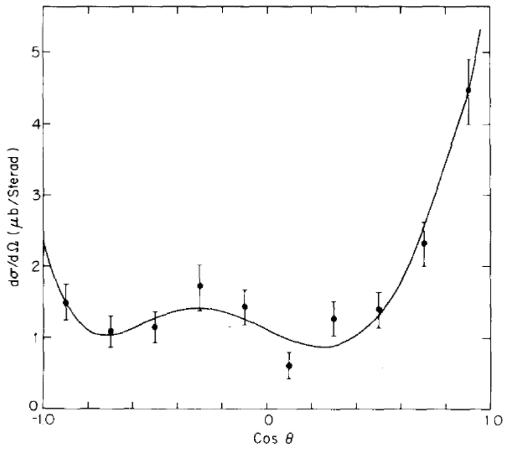


Figure 4: The differential cross section for $\pi^- p \to \Lambda(1405)K^0$[18]. The curve is a fit with Legendre polynomial.

### 3.1 $\bar{\mathrm{K}}$ bound state production via a $\Lambda(1405)$ doorway

The formation of $\bar{\mathrm{K}}$ bound states through the $\Lambda(1405)$ production as a doorway was first discussed by Yamazaki and Akaishi for the $(K^-, \pi^-)$ reaction[6]. The same idea should be valid for other strangeness-transfer reactions; $(\pi^+, K^+)$, $(K^-, N)$, and $(\gamma, K^+)$ [7]. They treated the formation of $\bar{\mathrm{K}}$ clusters by a $\Lambda^*$ doorway model, in which a $\Lambda^*$ produced in an elementary process, $\pi^+ + n \to \Lambda^* + K^+$, merges with a surrounding nucleon to become a $\bar{\mathrm{K}}$ state(see Fig. 5).

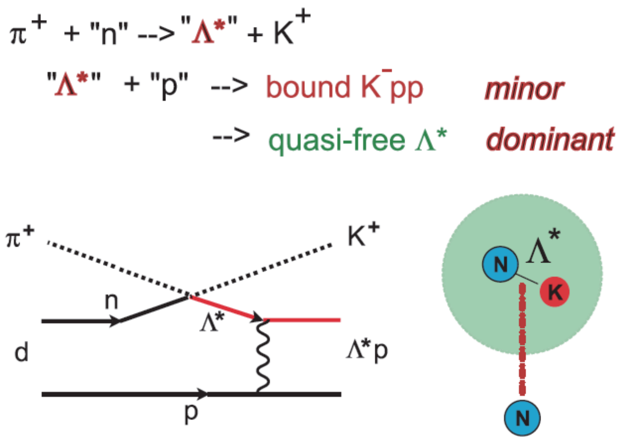


Figure 5: Diagram for the $d(\pi^+, K^+)K^-pp$ reaction[7].

The energy spectrum involving both the bound and unbound regions was calculated following the Morimatsu-Yazaki procedure[20]. It is given by

$$\frac{d^2\sigma}{dE_{K^+} d\Omega_{K^+}} = \alpha(k_{K^+}) \frac{d\sigma^{elem}_{\Lambda^*}}{d\Omega_{K^+}} \frac{|\langle \phi_{\Lambda^*} | v^{I=0}_{\bar{K}N} | \phi_{\Lambda^*} \rangle|^2}{\tilde{E}^2 + \frac{1}{4}\Gamma^2_{\Lambda^*}} S(E)$$

with a spectral function

$$S(E) = (-\frac{1}{\pi})\text{Im}\left[\int d\vec{r}_K d\vec{r}'_K \tilde{f}^*(\vec{r}_K) \times \langle \vec{r}_K | \frac{1}{E - H_{K^-pp} + i\epsilon} | \vec{r}'_K \rangle \tilde{f}(\vec{r}'_K)\right],$$

where $\tilde{E}$ is the energy transfer to the $\Lambda^*-p$ relative motion in doorway states, $E$ is the energy transfer to the $K^-pp$ relative (internal) motion in the $K^-pp$ system, and $\alpha(k_K^+)$ is a kinematical factor. The function $\tilde{f}(r)$ is

$$\tilde{f}(\vec{r}) = 2^3 e^{i2\beta\vec{q}\vec{r}} C(r)\Phi^*_{pp}(2r)\Psi_d(2r)/|\phi_{\Lambda^*}(0)|,$$

with $\vec{q} = \vec{k}_{\pi^+} - \vec{k}_{K^+}$, $\beta = M_p/(M_{\Lambda^*} + M_p)$, and $C(r) = 1 - \exp[-(r/1.2\text{fm})^2]$ and $\Phi_{pp}$ is the $p-p$ relative wave function in $K^-pp$. The calculated spectral function is shown in Fig. 6 for the $d(\pi^+, K^+)K^-pp$ reaction at 1.5 GeV/$c$.. The dominant part is the quasifree $\Lambda^*$ component in which the produced $\Lambda^*$ escapes, and a small fraction of the order of 1% constitutes a bound-state peak. Here, they assumed the $K^-pp$ has a binding energy of 86 MeV and a width of 58 MeV.

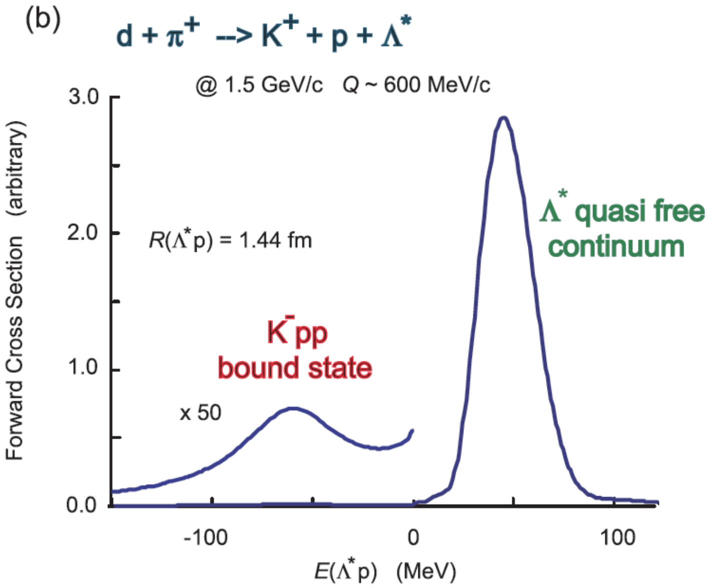


Figure 6: A calculated spectrum shape of the $d(\pi^+, K^+)K^-pp$ reaction[7].

## 4 Background

Since we use $\pi^+$ beam rather than $K^-$, decay-in-flight backgrounds are negligible.

However, we have a lot of physical background modes in quasi-free processes; (a) productions of $\Lambda$ and $\Sigma$ hyperons, (b) productions of $\Lambda + \pi$ and $\Sigma + \pi$ emitted in the three-body phase space, and (c) productions of other hyperon resonances like $\Sigma(1385)$ and $\Lambda(1520)$. The process (a) includes,

$$\begin{aligned} \pi^+ + d &\rightarrow \Lambda + K^+ + p_s, \\ \pi^+ + d &\rightarrow \Sigma^0 + K^+ + p_s, \\ \pi^+ + d &\rightarrow \Sigma^+ + K^+ + n_s, \end{aligned}$$

where the subscript $s$ indicates the spectator nucleon in the quasifree process. The total production cross sections in these modes are 100 – 250 $\mu$b. However, the forward $K^+$ momenta are above 0.9 GeV/$c$, and are well separated from the signal $K^+$ (see Fig. 7). The most serious background modes are the three-body quasifree processes (b) which include,

$$\begin{aligned}
\pi^+ + d &\rightarrow \Lambda + \pi^0 + K^+ + p_s, \\
\pi^+ + d &\rightarrow \Sigma^0 + \pi^0 + K^+ + p_s, \\
\pi^+ + d &\rightarrow \Sigma^- + \pi^+ + K^+ + p_s, \\
\pi^+ + d &\rightarrow \Sigma^+ + \pi^- + K^+ + p_s, \\
\pi^+ + d &\rightarrow \Lambda + \pi^+ + K^+ + n_s, \\
\pi^+ + d &\rightarrow \Sigma^+ + \pi^0 + K^+ + n_s, \\
\pi^+ + d &\rightarrow \Sigma^0 + \pi^+ + K^+ + n_s.
\end{aligned}$$

The total production cross sections in these modes are $50-80$ $\mu$b for each. The forward $K^+$ momenta overlap almost completely with the signal $K^+$ (see Fig. 7). As mentioned in the previous section, the quasi-free $\Lambda(1405)$ production cross section is the same order with the $\Sigma\pi K^+$ modes. The quasifree $\Sigma(1385)$ production could contribute to the inclusive $(\pi^+, K^+)$ spectrum. However, the cross section at very forward angles eventually drops off as measured in [18].

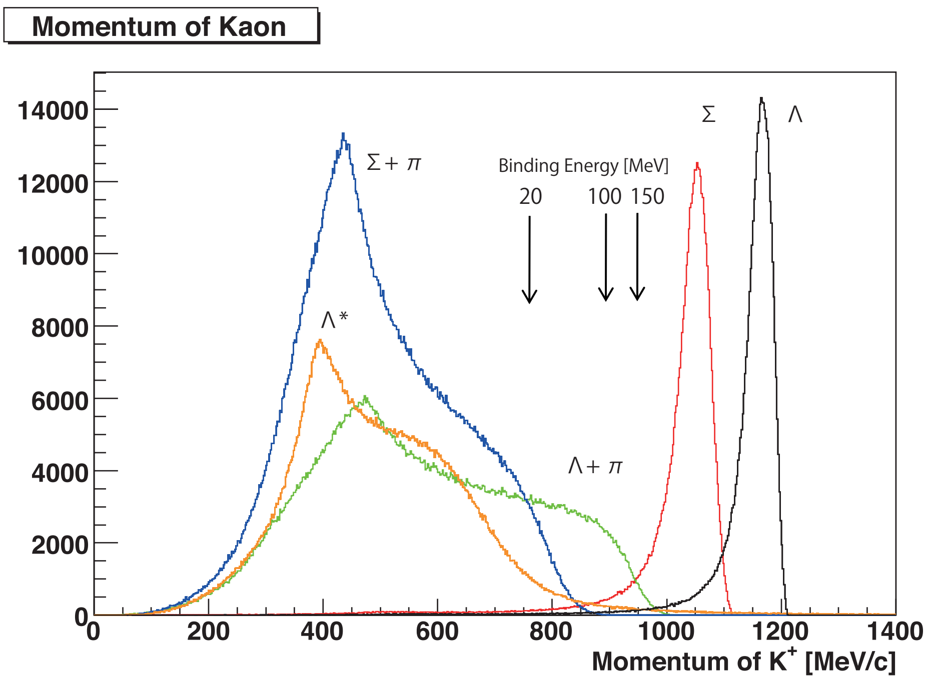


Figure 7: A simulated $K^+$ spectrum shapes for a various quasifree background processes (see text). Here the production cross sections at forward are assumed to be same for each process. The $K^-pp$ bound region is indicated by the arrows corresponding to the binding energies of 20, 100, and 150 MeV.

# 5 Experimental Procedure

## 5.1 Experimental Setup

We are going to use almost the same experimental setup (Fig. 8) in J-PARC E19 (Spokesperson: M. Naruki) for the $(\pi^+, K^+)$ missing-mass measurement. At the K1.8 beam line in the Hadron Experimental

Hall, we will use the $\pi^+$ beam at 1.5 GeV/$c$ analyzing the incident momentum particle by particle with a beam line spectrometer system. The emitted $K^+$ is momentum analyzed with the Superconducting Kaon Spectrometer (SKS).

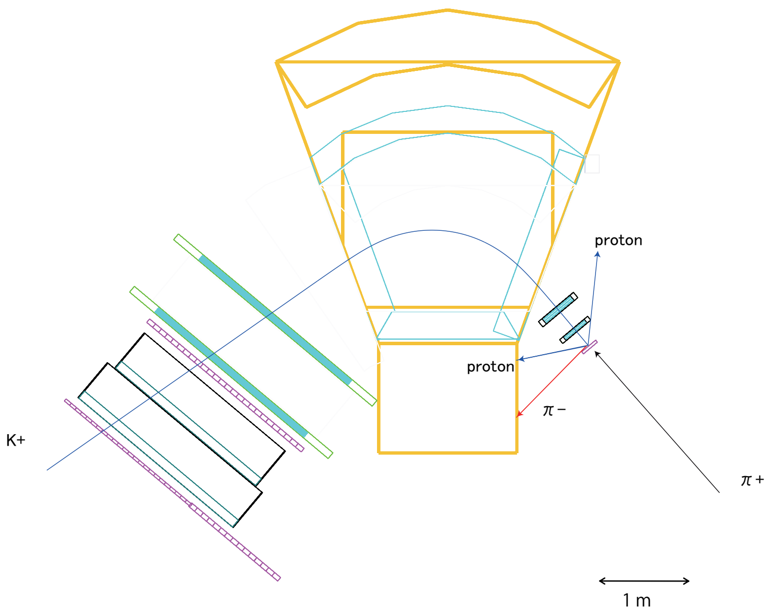


Figure 8: Experimental setup of J-PARC E19. A typical event pattern of $d(\pi^+, K^+)K^-pp$ is shown.

The reaction used is $\pi^+ + d \rightarrow K^+ + K^-pp$ at 1.5 GeV/$c$ in this measurement instead of $\pi^- + p \rightarrow K^- + \Theta^+$ at $\approx$1.9 GeV/$c$ in E19. The experimental target is replaced with liquid deuterium instead of liquid hydrogen in E19 in the same target cooling system.

In the typical $(\pi^+, K^+)$ run for $\Lambda$ hypernuclei, the incident pion momentum is 1.05 GeV/$c$ with the outgoing $K^+$ momentum of 0.72 GeV/$c$ and the momentum transfer is $\sim$0.35 GeV/$c$. In this experiment, the momentum transfer is larger ($\sim$0.6 GeV/$c$), then the outgoing $K^+$ momentum is almost in the same range ($\sim$0.85 GeV/$c$). Thus, the magnetic setting of the SKS magnet does not change so much. The expected energy resolution in the $(\pi^+, K^+)$ spectrum is 2.5 MeV (FWHM), which is enough for the present purpose.

In addition to this standard SKS spectrometer, we need to construct a proton tagging counter system surrounding the target in order to remove the three-body background processes.

## 5.2 Proton Tagging

The decay mode of the $K^-pp$ bound state is not known very well. If the binding energy is less than $\sim$100 MeV, the main decay mode of $K^-pp \rightarrow \Sigma\pi N$ is open. While even in that case it is expected that non-mesonic decay modes have significant contributions of the order of 10%. In fact, the experimental signals in the previous measurements are based on a $\Lambda + p$ decay mode.

In the non-mesonic decay modes, the $Q$-values are very high, $\geq$ 200 MeV, so that a hyperon and a nucleon are emitted with high momentum, $\geq$ 250 MeV/$c$. Another nucleon from the hyperon decay, $Y \rightarrow N + \pi$, also has high momentum because of the heavy mass.

The $K^-pp$ can decay in the non-mesonic decay as,

$$\begin{aligned} K^-pp &\rightarrow \Lambda + p, \\ &\rightarrow \Sigma^0 + p, \Sigma^0 \rightarrow \Lambda + \gamma \\ &\rightarrow \Sigma^+ + n. \end{aligned}$$

Therefore, in the first two decay modes, we can detect two protons in the final state, when the $\Lambda$ decays into a proton and a $\pi^-$ (64%). In Fig. 9, the correlation of two-proton momenta in the $K^-pp\rightarrow \Lambda + p$, $\Lambda \rightarrow p + \pi^-$, decay is shown. We can safely set the proton momentum threshold to 250 MeV/$c$.

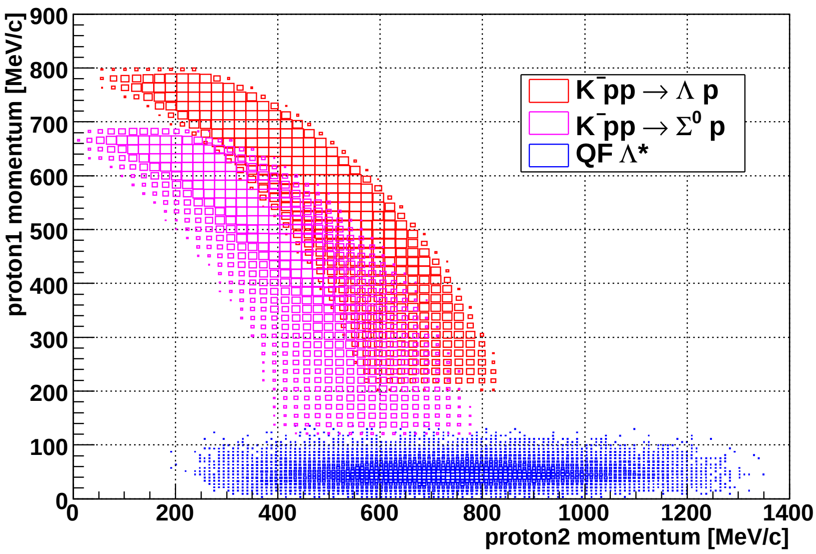


Figure 9: Correlations of the momenta of two protons; red squares correspond to the two protons from the decay mode of $K^-pp\rightarrow \Lambda p$, magenta squares for $K^-pp\rightarrow \Sigma^0 p$, and blue ones for the quasifree $\Lambda^*$ production.

On the contrary, in the main background mode of quasi-free three-body hyperon productions, $\pi^+ + d\rightarrow K^+ Y\pi + p_s$, there could be only one high-momentum proton from the decay of a hyperon and the spectator proton momentum is smaller than the proton momentum threshold. Therefore, we can remove all the quasi-free background by requiring two high-momentum protons in the final state.

## 5.3 Proton Range Counter

We need to identify two high-momentum ($\geq$250 MeV/$c$) protons separated from slow ($\leq$250 MeV/$c$) pions. For this purpose, we use range and velocity measurements. The range is measured with an array of plastic scintillators. The array consists of five blocks of plastic scintillators. Each block of plastic scintillators has four layers of plastic scintillators with the size of 10 cm[W]$\times$100 cm[L] and the different thicknesses of 0.3 cm, 1 cm, 2 cm, and 5 cm, respectively. We have two arrays placed at both sides of the beam direction covering from 40 degrees to 80 degrees with the 50-cm distance from the target center. The flight time is measured with the plastic scintillator having the start timing of a thin plastic scintillator hodoscope surrounding the deuterium target vessel with the 15-cm distance from the target center. A conceptual design of the hodoscope system is shown in Fig. 10.

With this setup, the detection efficiency of two protons in coincidence in the decay mode of $K^-pp\rightarrow \Lambda + p$, $\Lambda \rightarrow p + \pi^-$, is estimated to be about 14% with the proton momentum threshold of $\sim$250 MeV/$c$ including the solid-angle acceptance. Please note that the two protons are emitted almost back-to-back in the lab. frame.

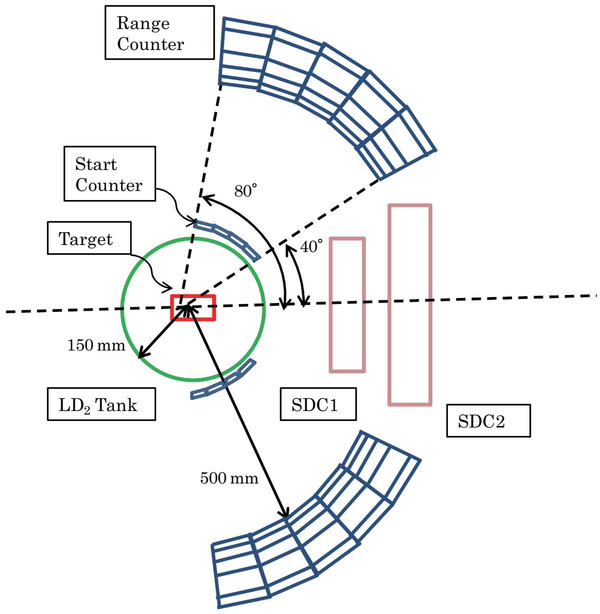


Figure 10: A conceptual design of the range hodoscope detector system.

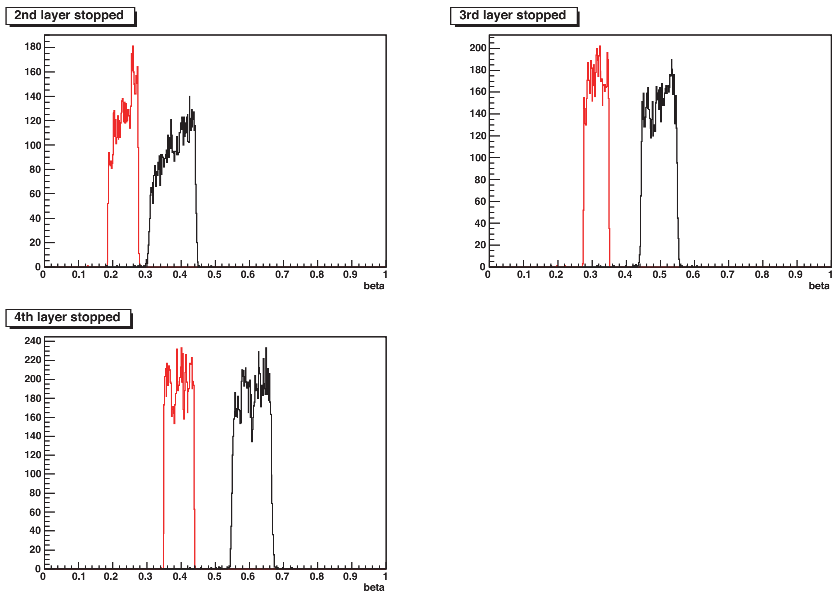


Figure 11: Particle identification of proton and pion. The particle velocity($\beta$) distributions for pions(red) and protons(black) are shown for three different stopping layers in the range counter.

### 5.4 Yield Estimation

The total yield of the $\Lambda(1405)$ production in one day of data taking is estimated to be

$$5 \times 10^6[\pi^+/spill] \times 1000[spills/hour] \times 20[hours/day] \times 60 \times 10^{-30}[cm^2/sr] \times 0.1[sr]$$
$$\times \frac{N_A}{2}[/g] \times 1.4[g/cm^2] \times 0.5_{decay} \times 0.5_{track} = 6.3 \times 10^4 events/day.$$

Here, we have used the $\Lambda(1405)$ production cross section at forward angles to be 60 $\mu$b/sr in the lab. frame, 100 msr for the SKS acceptance, 1.4 g/cm$^2$ for the amount of liquid deuterium, a $K^+$ decay factor of 0.5, and an overall tracking efficiency for the $K^+$ to be 0.5. Then, if we assume that 1% of the produced $\Lambda(1405)$ are trapped to form the $K^-pp$, the non-mesonic decay branch of the $K^-pp$ is 20%, the two-proton emission probability is 2/3($\Lambda$ and $\Sigma^0$ among $\Lambda/\Sigma^0/\Sigma^+$) $\times$ 2/3($\Lambda$ to $p + \pi^-$ branching fraction), and the detection efficiency for two protons in coincidence is 14% including the solid-angle acceptance, we can estimate the yield for two-proton events from the $K^-pp$ formation is

$$6.3 \times 10^4 \times 0.01 \times 0.2 \times \frac{2}{3} \times \frac{2}{3} \times 0.14 = 7.8 events/day.$$

Therefore, in the data taking of 40 days, we can have about 300 events of signals.

### 5.5 Cost Estimation

In addition to the standard $(\pi^+, K^+)$ setup of the SKS spectrometer system at K1.8 beam line, we require the deuterium target and the range hodoscope counter. These costs are roughly estimated in Table 1

Table 1: Cost estimation

| *Item* | *Cost in 1,000 yen* |
|---|---|
| Deuterium gas (3,000$\ell$) | 900 |
| Range Hodoscopes | |
| - Scintillators 100 cm×10 cm× 0.3 cm×10 | 200 |
| - Scintillators 100 cm×10 cm× 1 cm×10 | 300 |
| - Scintillators 100 cm×10 cm× 2 cm×10 | 400 |
| - Scintillators 100 cm×10 cm× 5 cm×10 | *existing at KEK* |
| - Scintillators 30 cm×4 cm× 0.2 cm×10 | 50 |
| - PMT H6410 ×80 | *to be obtained at KEK* |
| - PMT R3478s ×20 | 1,200 |
| - Support frames × 3 | 1,000 |

## 6 Future Program

Once the existence of such a $K^-pp$ bound system is confirmed, we can proceed to the $^3$He$(\pi^+, K^+)K^-ppp$ reaction, where a strongly bound $K^-ppp$ system with the binding energy of ∼100 MeV or more will be produced. According to Doté *et al.*[21], the $K^-ppp$ system has a very peculiar density distribution as shown in Fig. 12. Here, one proton is located as a satellite, while the remaining part forms the $K^-pp$ configuration. Two-proton tagging method might work for this case to remove the quasifree background processes, although we have a large ambiguities on the decay property of $K^-ppp$.

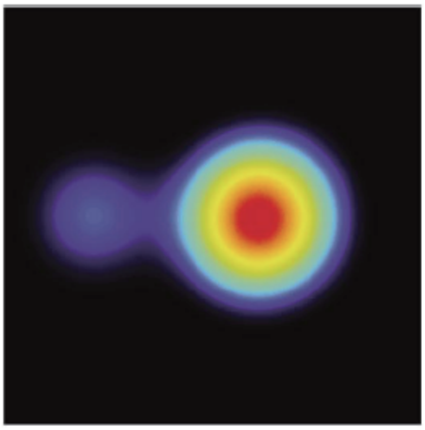

pppK$^-$

Figure 12: Density contour of the nucleon distribution for $K^-ppp$: 3 fm $\times$ 3 fm.

# 7 Summary

We will use the $d(\pi^+, K^+)$ reaction to search for a $\bar{\mathrm{K}}$ bound state of $K^-pp$. Within 40 days of data taking, we can acquire about 300 events of the $K^-pp$ production signal in the $(\pi^+, K^+)$ missing-mass spectrum in a background free condition by requiring two high-momentum protons in the target region. Together with five days of detector tuning and calibrations, we can complete the measurement in one and a half months. The requirement on the intensity of the slow-extraction proton beam is modest; we need the $\pi^+$ intensity on the experimental target to be $5\times10^6$/spill at 1.5 GeV/$c$.

# References


[1] M. Agnello *et al.*, Phys. Rev. Lett. **94** (2005) 212303.

[2] H. Fujioka for the FINUDA group, oral presentation at PANIC08.

[3] V.K. Magas, E. Oset, A. Ramos, and H. Toki, Phys. Rev. C **74** (2006) 025206.

[4] N.V. Schevchenko, A. Gal, and J. Mareš, Phys. Rev. Lett. **98** (2007) 082301; Phys. Rev. C **76** (2008) 044004.

[5] Y. Ikeda and T. Sato, Phys. Rev. C **76** (2007) 035203; Y. Ikeda and T. Sato, Phys. Rev. C **79** (2009) 035201.

[6] T. Yamazaki and Y. Akaishi, Phys. Lett. B **535** (2002) 70.

[7] T. Yamazaki and Y. Akaishi Phys. Rev. C **76** (2007) 045201.

[8] A. Doté, T. Hyodo, and W. Weise, Nucl. Phys. A **804** 197; Phys. Rev. C **79** (2009) 014003.

[9] A. Arai, M. Oka, and S. Yasui, Prog. Theor. Phys. **119** (2008) 103.

[10] N. Herrmann, Proc. of EXA05, A. Hirtl *et al.* Eds., Austrian Academy of Science Press, Vienna, 2005, pp. 73-81.

[11] G. Bendiscioli *et al.*, Nucl. Phys. A **789** (2007) 222.

[12] T. Yamazaki *et al.*, arXiv:nucl-ex/0810.5182 (to appear in the Proc. of EXA08).

[13] Y. Nogami, Phys. Lett. **7** (1963) 288.

[14] M.H. Alston *et al.*, Phys. Rev. Lett. **6** (1961) 698.

[15] Y. Akaishi and T. Yamazaki, Phys. Rev. C 65 (2002) 044005.

[16] Y. Akaishi and T. Yamazaki, Proc. DAΦNE Workshop (November 16-19, 1999), Frascati Physics Series Vol. XVI, pp59-74..

[17] Y. Akaishi and T. Yamazaki, Nucl. Phys. A 684 (2000) 409c.

[18] D.W. Thomas *et al.*, Nucl. Phys. **B56** (1973) 15.

[19] R.J. Hemmingway *et al.*, Nucl. Phys. B **253** (1985) 742.

[20] O. Morimatsu and K. Yazaki, Nucl. Phys. **A435** (1985) 727.

[21] A. Doté, H. Horiuchi, Y. Akaishi, and T. Yamazaki, Phys. Rev. C **70** (2004) 044313.